Journal of Environmental Science and Engineering, 5 (2011) 453-459

Heat and Radiation Generation during Hydrogenation of CH Compound

T. Mizuno[1]

Hydrogen Engineering Application & Development Company, Korabo Hokkaido G-room, Kita-ku, Kita21 Nishi2, Sapporo 001-0021, Japan

Received: February 25, 2011 / Accepted: April 1, 2011 / Published: August 20, 2011.

Abstract: Securing new sources of energy has become a major concern, because fossil fuels are expected to be depleted within several decades. In some of the major wars of the 20th century, control of oil was either a proximate cause or a decisive factor in the outcome. Especially in Japan and Germany, a great deal of research was devoted to making liquid fuels from coal. In one such experiment, a large amount of excess heat was observed. The present study was devoted to replicating and controlling that excess heat effect. The reactant is phenanthrene, a heavy oil fraction, which is subjected to high pressure and high heat in the presence of a metal catalyst. This results in the production of excess heat and strong penetrating electromagnetic radiation. After the reaction, an analysis of residual gas reveals a variety of hydrocarbons, but it seems unlikely that these products can explain the excess heat. Most of them form endothermically, and furthermore heat production reached 60 W. Overall heat production exceeded any conceivable chemical reaction by two orders of magnitude.

Key words: Heat generation, hydrogen, carbon, catalyzer.

1. Introduction

Numerous studies concerning the hydrogenation of hydrocarbons have been performed to date. The hydrogenation reaction of naphthalene using zeolite supported Pd and Pt catalysts at low temperature was examined by Song et al. [1]. In particular, they investigated the effects of catalytic poisoning by sulfur. The H_2 transfer reaction between phenanthrene and H_2 in the presence of K/MgO in temperatures between 250 to 350 °C was studied by Fedorynska et al. [2]. Hydrogenation of phenanthrene using Raney Ni and CuCrO within the temperature range of 370 to 573K was tried by Durland et al. [3]. The pioneering work of hydrogenation of phenanthrene around 227 °C under 136-218 atm of hydrogen gas was began by Burger et al. [4]. An alumina supported Pt and Pd catalyst was used by Qian et al. [5] for the hydrogenation of phenanthrene, and they obtained a conversion rate that approached 100%. Another electro-catalytic hydrogenation technique that provided a comparably high conversion rate was developed by Mahdavi et al. [6, 7] and Chapuzet et al. [8].

This study was stimulated by above studies of a liquefying reaction to change the heavy oil to light oil. Abnormal heat generation was observed during the hydrogenation experiments when heated in high-pressure hydrogen gas. The amount of heat generated was abnormally large considering the expected chemical reaction between a few drops of heavy oil and a little hydrogen gas. Based on their estimate, they concluded the heat generated had not come from a conventional chemical reaction. However, they have not publicized any papers and references.

2. Experiment

2.1 Reaction Cell

Corresponding author: T. Mizuno, Ph.D., main research fields: nuclear physics, electrochemistry, metallurgy, condensed matter physics.
E-mail:mizuno@qe.eng.hokudai.ac.jp.

Fig. 1 shows a schematic of the reaction cell and the experimental set up. The reaction chamber is cylindrical. It is constructed from Inconel 625. It has a 16-mm outer diameter, a 10-mm inner diameter, a 300-mm height, and has a 0.01 L capacity. It can sustain a pressure of 500 atm, and it can be heated to 850 °C. The reactor has a plug for the hydrogen inlet and outlet, and housing for an internal temperature sensor. A platinum catalyst is placed inside the cell. The temperature inside the cell is measured with an R-type thermocouple, 1.6 mm in diameter, 30 cm long, which is enveloped in a 0.3 mm thick SS314 stainless steel shield and grounded to reduce noise. The thermocouple range is from -200 to 1,300 °C. Moreover, another thermocouple of the same type is inserted between the outer reactor wall and the inner wall of the electric furnace, to measure the temperature of the outside wall of the reactor cylinder. Thermocouple data is collected by a data logger (Hewlett Packard HP3497A), with a temperature sensitivity of 0.1 °C. The error ranges of the temperature measurement system is determined by the resistivity of the thermocouples (4 Ω), the insulation (100 MΩ), and the data logger (100 MΩ). In this case, the error works out to be 0.03% of the instrument reading. At a temperature of 800°C the error is 0.03 °C.

2.2 Measurement System

As shown in Fig. 1, the cell is placed in the electric furnace, and hydrogen gas is introduced into the cell through a 6 mm diameters stainless steel pipe. The pipe is fitted with high pressure Swagelok valves which are used to introduce gas into the cell, or to evacuate it. Hydrogen is stored in a tank at 135 atm. It passes through a piezoelectric pressure transducer (Kyowa P-100KA) and amplifier (Shinko Tsushin 603F) and the flow rate is recorded in the data logger. Gas purity is more than 99.999%. The gas line is connected to the vacuum pump and mass spectrometer (ULVAC REGA201) that detects mass numbers up to 400.

The electric furnace is custom made (Tokyo Technical Lab. PH, Mo13763A1). It is 200 mm outside diameter, 65 mm inside diameter and 200 mm high. A direct current regulated power supply is used (Takasago Electric EX-1500H), that produces up to 240 V at 6 A (1.5 kW). The heater power is monitored

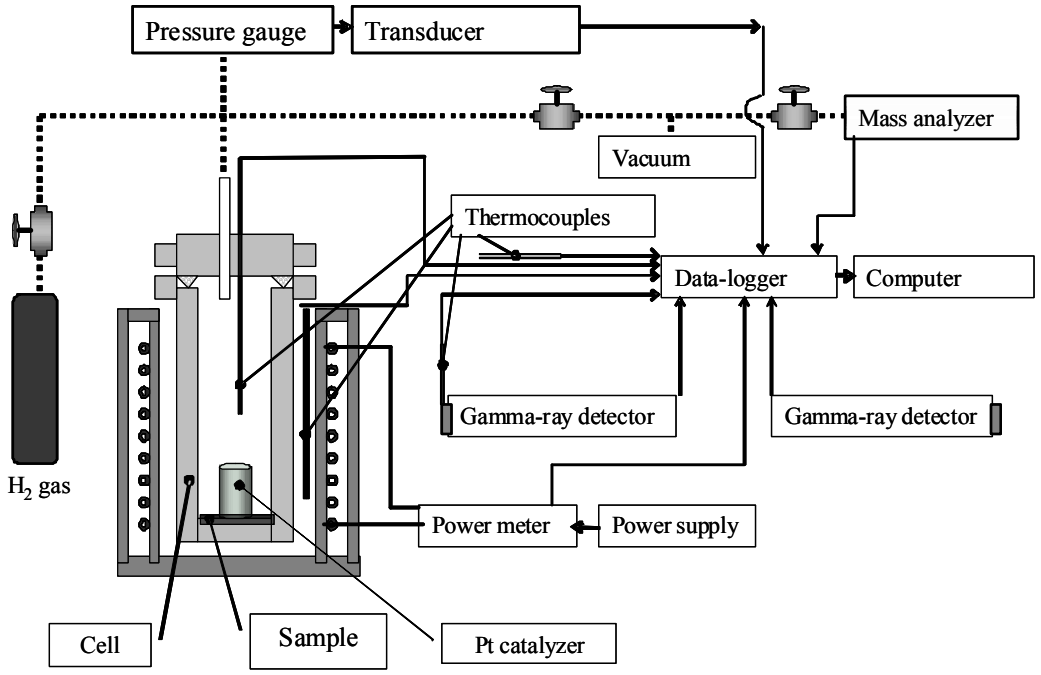

Fig. 1 Schematic drawing for the experimental set up.

with high precision meter (Yokogawa PZ4000), which measures amperage and voltage every millisecond, sending averaged data to the data logger at 5-second intervals. The combined error for amperage and voltage is 0.0015%.

Radiation emissions are detected by a γ-ray detector (Aloka ICS-311) that is located 15 cm from the reactor. Its output is recorded continuously by the computer through a digital multimeter (Advantest TR-6845). The ionization chamber has a 14 cm long electrode, a correction plate 1 cm long, a window 0.5 cm thick, and it is pressurized with air at 1 atm. This detector can detect x-rays, γ-rays and β-rays. It can detect x-rays and γ-rays in the range of 30 keV ~ 2 MeV with an efficiency of 0.85 ~ 1.15 calibrated with ^{137}Cs. The measurement range dose equivalent rate at 1 cm is 1 mSv/h ~ 10 mSv/h. The response time is less than 5 s. The device is powered with a lithium battery. These characteristics make the device highly accurate and stable over long periods of time.

With this detector chamber, where the number of incident photons per unit of time is n (s^{-1}), and the energy is E (eV), and the percentage of energy converted to the signal inside the chamber is ε, the unit charge is e (1.6×10^{-19} C) the signal current i (A) is: $i = n \varepsilon Ee/W$.

Thus, when the chamber is filled with air, $n = 10^{10}$ photons/s, ε = 0.9, E = 10 keV, W = 35 eV, $i = 4.1 \times 10^{-7}$ A. The output signal voltage is proportional to the incident photo intensity. At 1 mSv/h, output is 30 mV. This output is sent to the data logger and recorded in the computer. The detection of radiation emission employed a gamma-ray detector, which was calibrated by a 3.7×10^5 Bq ^{226}Ra check source that was positioned at various distances from the gamma-ray detector. Before the experiment, the check source was placed inside the reactor cylinder to obtain a gamma-ray reading. The background radiation level surrounding the system was 0.05 ± 0.008 μSv/h.

The radiation data was further processed with OriginPro software (OriginLab) to analyze multiple peaks. A Gaussian distribution analysis was performed to fit of multiple peaks, with the following equation:

$$y = y_0 + A(w(\pi/2)^{-1/2})\exp(-2(x-x_0)^2/w^2) \quad (1)$$

Where:

y_0 = Baseline offset;

A = Total area from baseline to curve;

X_0 = Midpoint of peak;

W = 2σ. Full width at half maximum = 0.849;

The midpoint X_0 is the average, where w/2 is the standard deviation.

To reduce the difference between the fitted curve and original data, additional peaks were plotted, and the following peak analysis was performed. To analyze multiple peaks, a function with multiple dependent variables and independent variables was defined in the following equations:

$y_1 = f(x_1, x_2, ..., a, b, c, ...)$

$y_2 = f(x_1, x_2, ..., d, e, f, ...)$

……

$y_n = f(x_1, x_2, ..., o, p, q, ...)$

Here, x_1, x_2, … x_n are independent variable and a, b, c,…o, p, q are coefficient for the variables.

The Gaussian peaks derived with these functions are closest to the original data.

2.3 Materials

Fluorescent grade (98.0% pure) phenanthrene ($C_{14}H_{10}$: MW 178.23) was used in this study. It was supplied by the Kanto Chemical Co. LTD. The Pt catalyst was a high purity (99.99%) Pt mesh (Tanaka Noble Metal Co. LTD.). The catalyst is rectangular and is 5 cm high, is 10 cm wide, and weighs 50 g. Before the experiment, the Pt catalyst was activated once in an atmosphere of hydrogen gas for 1 hour at 850 °C.

2.4 Experimental Procedures

One gram of phenanthrene and the Pt catalyst were put in the reactor; the reactor cell was then sealed with the lid, which was secured in place with bolts. The reactor was connected to the vacuum system and evacuated to 10^{-3} mmHg. The vacuum system exhaust

valve was left open for several minutes to remove the residual air from the reactor. The exhaust valve was then closed, and the gas was supplied to the reactor at the set pressure. After gas filled the reactor, the gas supply valve was closed. The temperature of the gas in the reactor then was increased to the starting temperature. Calibration of temperature versus pressure was performed by changing the hydrogen gas pressure from a vacuum to 80 atm.

2.5 Temperature Calibration

The amount of excess heat is determined by comparing input heater power to a stable temperature in the cell on a calibration curve. Fig. 2 shows the relationship between heater power and the cell temperature. These data points were taken with the phenanthrene sample in the cell but no Pt catalyst present. They were taken after the temperature stabilizes: the values shown are cell temperature minus ambient temperature. To arrive at a stable temperature, the heater has to be set at a fixed power level for about 83 minutes. This graph shows data taken at various gas pressures. The conductivity of hydrogen gas from 10^{-3} to 10 atm is almost constant. However, above 10 atm conductivity increases and the average temperature of the gas falls. The relation between the temperature and input power is not linear in a log-log scale above 550 °C, but the curves for different pressure settings all have similar declines above this temperature. In this experiment, the highest temperature achieved was 800 °C.

The relationship between temperature (T) and furnace heater input power (W) is represented by a simple equation, $T = CW^k$, within this temperature region. The exponent k is nearly constant, 0.60, for all calibration conditions. The heat conductivity of hydrogen ranges from 0.18 to 0.42 W $m^{-1}\cdot K^{-1}$ from 373 to 1273 K, respectively, and is almost constant within the pressure range from 1 to 100 atm [9]. However, as shown in Fig. 2 in the high pressure domain as gas pressure increases thermal conductivity and heat dissipation increase. The radiant heat loss is expressed by the relationship below.

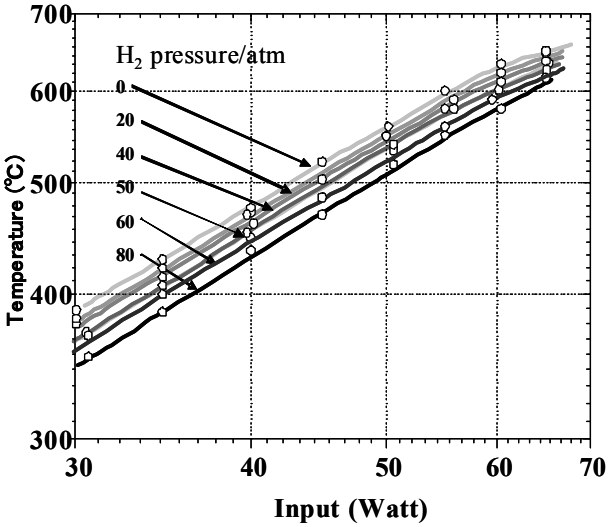

Fig. 2 Temperature dependence on heater power at different H_2 gas pressures.

The relationship is nonlinear and the coefficient k is 0.6 because the process of heat release is dependent on the heat conductivity and the radiant constant. Especially, the thermal conductivity increases with temperature. The heat release process by the radiant process becomes predominant in the high temperature region, as expressed by the following relationship:

$$P = \sigma\varepsilon A(T_s^4 - T_a^4)$$

Here, P is the heat lost ($W\cdot m^{-1}\cdot K^{-1}$), σ is the Stefan-Boltzmann constant (5.67×10^{-8} $W\cdot m^{-2}\cdot K^{-4}$), ε is the radiant constant, T_s is the absolute temperature of the body, and T_a is the surrounding temperature.

Fig. 3 (left) shows the change in gamma-ray emissions of the background. The intensity distribution is shown in Fig. 3 (right). Although it fluctuates around 0.05 μSv/h, the average of the background gamma-ray intensity is constant. The intensity distribution corresponds with a Poisson distribution, since the background is a Poisson process.

Fig. 4 (left) shows the change in gamma-ray emissions with a 0.1 μCi (3.8 kBq) ^{226}Ra source. This graph shows data over a 15.7 ks period. The check source was located 10 cm from the detector, except from 1.8 to 4 ks when the check source was positioned closer to the detector. The periods before 1.8 ks and

after 4 ks indicate the background gamma-ray emissions.

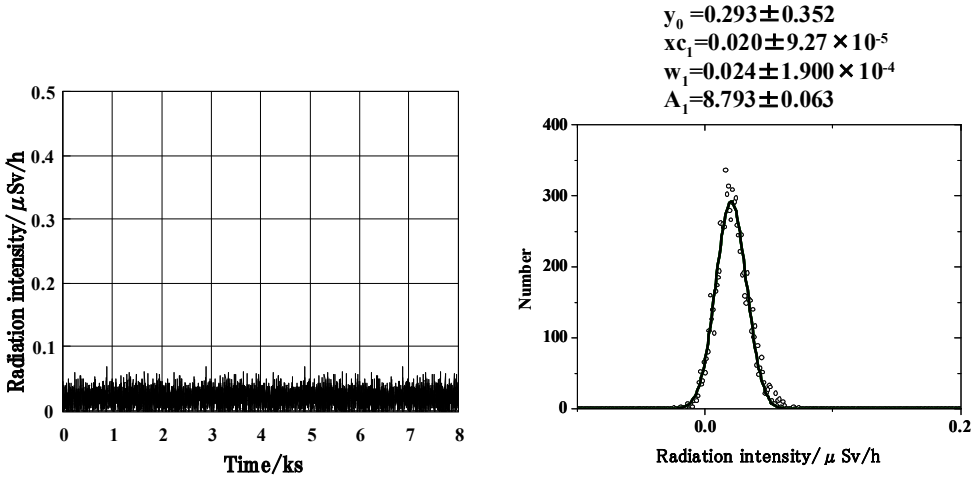

Fig. 3 (Left) Background change for γ -ray emissions. (Right) Intensity spectrum for the left graph.

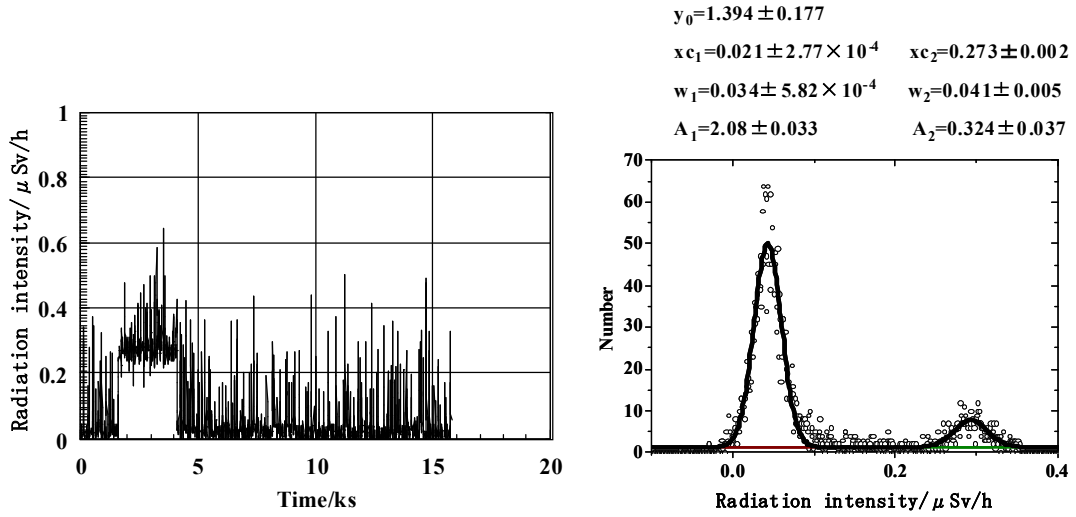

Fig. 4 (Left) A calibration whit a ^{226}Ra source placed 10 cm from the ionization chamber. (Right) Intensity distribution of the left graph.

The gamma-ray emissions increase six fold, from 0.05 to 0.3 μSv/h, when the isotope source was moved closer to the detector. The calibration of the gamma-ray emission detector was performed to change the set up time and distance to locate the source position from the detector by using a standard radiation source.

Fig. 4 (right) shows the intensity distribution of gamma-ray emissions from Fig. 4 (left). Two peaks are shown in this intensity distribution figure. These peaks at the 0.04 and 0.3 μSv/h positions are caused by the background and the source, respectively. The solid line in figure shows the calculated intensity distribution. In this case, the peak of the gamma-ray emission from the source clearly differs from that of the background.

However, when the position of the source was far from the detector and the data accumulation time was short, it is difficult to distinguish the foreground peak from that of the background. Some of the data points are distributed under than zero. This is caused the offset of the zero point of the detector. We calibrated the zero point in the background of the experimental room.

3. Results

3.1 Excess Heat Generation

Fig. 5 (left) shows an example of anomalous excess heat. In this test, 1 g of phenanthrene was exposed to a 70 atm of hydrogen gas. Furnace heater power was set for 60 W. The furnace heater temperature rose faster than the cell temperature. As shown in the calibration curve (Fig. 2) when there is no anomalous heat, by 10 ks both temperature stabilize at around 640 °C. However, in this test they both soon begin to rise above the stabilization point. After 5 ks, large perturbations begin and the temperatures continue rising. Also, at this point the cell temperature exceeds the furnace heater temperature. This temperature reversal is proof that heat was being produced inside the cell. The cell temperature reaches 800 °C, which is 200 °C higher than the calibration curve predicts. Since input power is 60 W, based on the curve in Fig. 2 we extrapolate that roughly 60 W of anomalous heat is being produced. Because of the extreme fluctuation in heat, total energy is more difficult to estimate than power, but because the excess power persisted for 10 ks it was at least 600kJ in this test.

Fig. 5 (right) shows the intensity distribution of gamma-ray emission from the ionization chamber detector. Two peaks are shown, 0.05 μSv/h and 0.09 μSv/h of the background by calculated peak analysis. These are clearly differentiated from the background of 0.02 μSv/h. Gamma-ray emissions were weak but they were clearly observed when intense excess heat was generated.

Total heat production can be estimated from the calibration curve and total duration of excess heat production which started around 18 ks and continued to 50 ks. Over this period, the average temperature was 50 °C above the calibration point continuing for 40 ks. Based on the calibration point of 600 °C (in Fig. 2) the excess was roughly 5 W on average, so total heat production was roughly 160 kJ for the entire run.

Fig. 6 (left) shows an example of a test with no excess heat. As in the test shown in Fig. 5, 1 g of phenanthrene was exposed to a 70 atm of hydrogen gas, and furnace heater power was set for 60 W. However, the Pt catalyst was not placed in the cell. By 10 ks, the temperature stabilized at about 600 °C. After that the temperature remained stable and settled.

Fig. 6 (right) shows the intensity distribution of gamma-ray emission for the test shown in Fig. 6 (left). Only the background peak is observed. Calculated peak analysis reveals no other peaks.

Fig. 7 shows various conditions under which heat is produced or not produced, and the associated radiation peaks relative intensity compared to the background. The 0.02 μSv/h peak is the background; the others are normalized to it. Even when there is no excess heat, in other words when the catalyst, hydrogen gas, or the phenanthrene sample is removed from the cell in a blank test, there is a peak 0.034 ~ 0.048 μSv/h. But, when there is excess heat, two peaks appear at the same time (at 0.04 and 0.09 μSv/h) and the intensity of the first one is stronger than the blank test peaks.

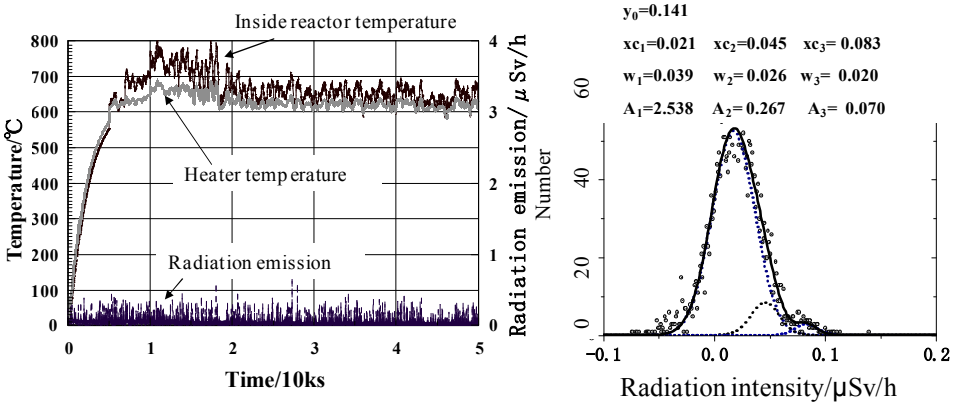

Fig. 5 (Left) An example of anomalous heat. (Right) Intensity spectrum for the left graph.

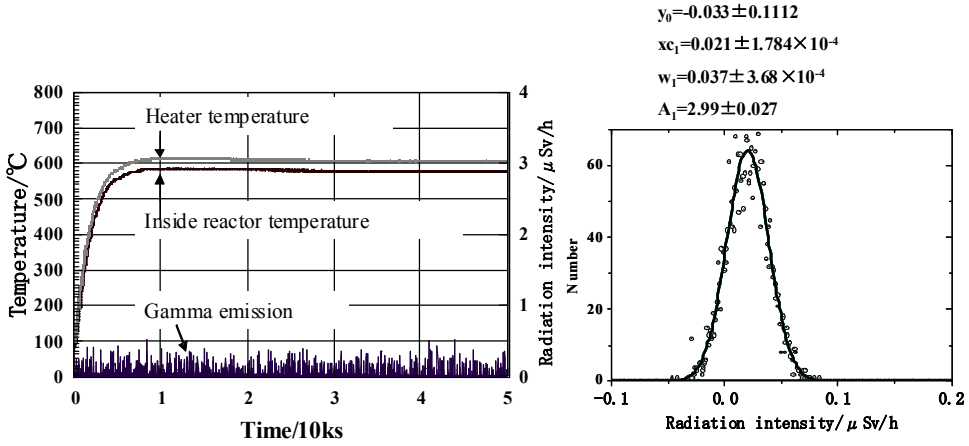

Fig. 6 (Left) An example with no anomalous heat. (Right) Intensity spectrum for the left graph.

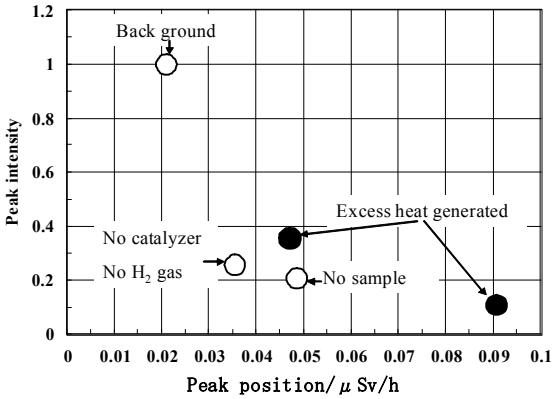

Fig. 7 The radiation emission peak position and intensity under various conditions.

Table 1 Conditions in various experiments.

Result	Conditions		
	Pressure (atm)	High temperature (Celsius)	Gas volume (L)
Excess heat produced	60	800 max	0.31
No excess heat	60	605	0.54
No catalyzer in cell	60	600	0.48
No sample	60	600	0.31
No H_2 gas in cell	0 (0.33)	350	0.01

3.2 Post Experiment Mass Spectra Analyses

Table 1 summarizes the results of post-experiment mass spectra analyses of the gasses removed from the cell after several experiments. Excess heat production (or no heat), and the presence or absence of the catalyst, sample and hydrogen gas are shown for various experiments and control experiments. When present, the phenanthrene sample was 1 g; the platinum catalyst was 27.8 g; and hydrogen gas was at 60 atm. The duration of most tests was 60 ks (16.6 hours) except when hydrogen gas was not present. Heater power was set to raise the cell temperature to 600 °C in the absence of excess heat. Spectra analyses were performed up to mass number 100.

When hydrogen gas was not present it was not possible to heat the cell as much. The highest temperature that could be reached was 350 °C. When the gas was present, in all tests pressure was set at 60 atm. When excess heat was not produced, the terminal temperature was always close to 600 °C. The last column in Table 1 shows the volume of gas produced in the cell. In nearly every case this ranged from 0.3 to 0.5 L.

Table 2 shows the results of the post-experiment analysis of the cell gasses. The detected species up to M/e 100 are shown in this table. Regardless of whether excess heat was produced or not the gas included 20~40% hydrogen, and about 30% each of CH_3 and CH_4. These three species together constituted 80% of the gas. Here, when excess heat is produced, 10% or more of the gas is what appears to be nitrogen (M/e = 28). However, nitrogen gas is usually remaining in the system due to the air leak into the measurement system. We conclude the M/e = 28 peak is caused from atmosphere.

When the catalyst is not present, 68% of the post-experiment gas is hydrogen, and CH_3 and CH_4 are

generated, both making up 12% of the gas. When there is no phenanthrene, obviously, no reaction occurs, and all of the gas is hydrogen. When there is no hydrogen to act as reactant, only C_2H_x, C_3H_x and other heavy hydrocarbons are found, indicating that a thermal decomposition reaction has occurred.

Table 2 The gas compositions after the test.

Mass number	Species	Excess heat	No excess heat	No catalyzer	No sample	No gas
2	H_2^+	21.00	37.0	68.00	96.20	13.00
12	$^{12}C^+$	0.70	0.70	0.30	0.00	3.70
13	$^{13}C^+$+CH^+	2.50	2.60	1.00	0.00	1.80
14	CH_2^+	3.80	1.00	1.60	0.36	1.10
15	CH_3^+	27.00	27.00	12.00	0.10	21.00
16	CH_4^+	28.00	34.00	12.00	0.10	7.50
17	OH^+	0.30	0.00	0.10	0.10	0.08
28	N_2^+	12.50	0.00	0.10	0.25	0.00
29	$C_2H_5^+$	0.10	0.10	0.10	0.10	11.00
43	$C_3H_7^+$	0.10	0.10	0.10	0.10	25.00
other		4.20	0.10	4.90	3.10	15.00

In the example shown in Table 1 with excess heat, 0.33 L of gas was produced, including 0.081 L of CH_3 and 0.087 L of CH_4, or 0.0036 and 0.0039 moles respectively. The chemical-bond enthalpies of these species are 146.6 and -74.9 kJ/mol, so the production of CH_3 is endothermic, consuming 5.27 kJ, and the CH_4 production is exothermic, producing 2.92 kJ. The overall reaction is endothermic, consuming 2.35 kJ [10, 11].

Furthermore, the heat of formation of phenanthrene ($C_{14}H_{10}$) can be determined from the enthalpies of the two elements C and H, and it comes to -2.82 MJ/mol. The heat of decomposition is the opposite; that is to say, endothermic. The sample is 1 g or 0. 0056 mol, so decomposition absorbs 15.8 kJ endothermically. The overall reaction is 18.2 kJ endothermic.

4. Discussion

In these experiments, a 1 g sample of phenanthrene was used, which is 5.6×10^{-3} moles. Oxidation, reduction and other chemical reactions can produce at most a few kilojoules from this much material, whereas this reaction produced on the order of 100 kJ of heat. That is roughly 100 times larger than a chemical reaction. Therefore, a chemical reaction as the source of this heat is conclusively ruled out. Furthermore, during the experiment weak radioactivity was observed, probably γ or x-rays. If these are γ-rays that is proof this is a nuclear reaction; if they are x-rays then they were generated by some other mechanism. The detector used in this study can detect an energy range starting from 20 keV up to high levels. The cell wall is 3 mm thick stainless steel. The x-ray mass absorbent coefficient for 20 keV x-rays is 100 cm^2/g, so most of the radiation would not penetrate the cell wall. However, if these are γ-rays at around 1 MeV, 80% of the radiation would pass through the cell wall. Therefore, although we cannot be certain it is very likely these are γ-rays.

The excess heat and radiation were not strongly correlated, but they both indicate that some sort of nuclear reaction occurred. With additional research to understand the mechanism of the reaction, this reaction might possibly become a practical source of energy.

5. Conclusions

The anomalous energy generation cannot be the product of a conventional chemical reaction for the following reasons:

(1) At these temperatures, hydrogenation reactions are endothermic, not exothermic;

(2) Based on this massive reaction and the mass of the reactants, the total heat release far exceeded any known chemical reaction;

(3) There was no chemical fuel in the reactor cells;

(4) There were no chemical reaction products. Except the platinum screen that was coated with carbon, the components and chemical species in the cell, including phenanthrene and hydrogen gas, remained essentially as they were when the experiment began;

(5) Gamma-ray emissions were detected. These emissions are characteristic of a nuclear reaction. These emissions might have been x-rays but this is unlikely.

The reaction is reliably triggered by raising temperatures above the threshold temperature of ~ 580 °C and hydrogen pressures above 60 atm. The reaction can be quenched by lowering the temperature inside the cell to below~ 500 °C. When the required conditions are satisfied excess heat is generated with high reproducibility, but the rate of heat production is not stable. There is only a small amount of reactant in the cell, and it is likely that the accompanying ordinary chemical reactions that occur in the cell soon consume it all.

Our findings are summarized as follows:

(1) Anomalous heat generation was confirmed during the heating of phenanthrene in high-pressure H_2 gas;

(2) Sporadic radiation emissions (probably gamma rays) were confirmed during the high temperature experiments;

(3) A weak correlation was observed between the anomalous heat generation and the radiation emissions.

Acknowledgements

The author would like to acknowledge financial support from the Hokkaido Gas Foundation in 2007, and from Mr. Brian Scanlan of Kiva Labs. The author would also like to express thanks to those who provided assistance, samples, analysis, and consultation in these experiments, including Mr. Hiroshi Yamakawa of Honda Technology Research, and Mr. Toshiyuki Sanpo, Dr. Yuji Yamauchi, Dr. Fumiyuki Fujita of the Department of Engineering, Hokkaido University. Finally, author would like to express thanks for the effort of translation to Mr. Jed Rothwell.

References

[1] C. Song, A.D. Schmitz, Zeolite-supported Pd and Pt catalysts for low-temperature hydrogenation of naphthalene in the absence and presence of benzothiophene, Energy & Fuels 11 (1997) 656-661

[2] E. Fedorynska, P. Winiarek, Influence of gaseous hydrogen on the hydrogen transfer reaction between phenanthrene and hydrogen donors, Reaction Kinetics and Catalysis Letters 63 (1998) 235-239

[3] J.R. Durland, H. Adkins, Hydrogenation of phenanthrene, Jornal of American Chemical Society 59 (1937) 135-137

[4] A. Burger, E. Mosettig, Studies in the phenanthrene series, 13. 9, 10–dihydro phenanthrene and amino alcohols derived from It, Journal of American Chemical Society 58 (1936) 1857-1860

[5] W. Qian, T. Yoda, Y. Hirai, A. Ishihara, T. Kabe, Hydrodesulfurization of dibenzothiophene and hydrogenation of phenanthrene on alumina-supported Pt and Pd catalysts, Applied Catalysis A: General 184 (1999) 81-88

[6] B. Mahdavi, J.M. Chapuzet, J. Lessard, The electrocatalytic hydrogenation of phenanthrene at raney nickel electrodes: The effect of periodic current control, Electrochimica Acta 38 (1993) 1377-1380

[7] B. Mahdavi, P. Los, M.J. Lessard, J. Lessard, A comparison of nickel boride and raney nickel electrode activity in the electrocatalytic hydrogenation of phenanthrene, Cannadian Journal of Chemistry 72 (1994) 2268-2277.

[8] J.M. Chapuzet, B. Mahdavi, J. Lessard, The electrocatalytic hydrogenation of phenanthrene at modified raney nickel electrodes, Journal de Chimie Physique 93 (1996) 1252-1261.

[9] I. Takagi, K. Toyoda, M. Katayama, H. Fujita, K. Higashi, Experiment on atomic hydrogen refection by use of a permeation probe, Journal of Nuclear Materials 258-263 (1998) 1082-1086.

[10] Y. Nagano, High-precision micro-combustion calorimetry of anthracene, The Journal of Chemical Thermodynamics 33 (2001) 377-387.

Y. Nagano, Standard enthalpies of formation of phenanthrene and naphthacene, The Journal of Chemical Thermodynamics 34 (2002) 377-383